BULLETIN OF THE POLISH ACADEMY OF SCIENCES
TECHNICAL SCIENCES, Vol. 62, No. 1, 2014
DOI: 10.2478/bpasts-2014-0012

Field test and numerical studies of the scissors-AVLB type bridge

W. KRASON and J. MALACHOWSKI*

Department of Mechanics and Applied Computer Science, Military University of Technology,
2 Gen. Sylwestra Kaliskiego St., 00-908 Warsaw, Poland

Abstract. Scissor bridges are characterized by high mobility and modular structure. A single module-span consists of two spanning parts of the bridge; two main trucks and the support structure. Pin joints are used between modules of the single bridge span. Some aspects of the experimental test and numerical analysis of the scissor-AVLB type bridge operation are presented in this paper. Numerical analyses, presented here, were carried out for the scissors-type BLG bridge with treadways extended as compared to the classical bridge operated up to the present in the Armed Forces of the Republic of Poland. A structural modification of this kind considerably affects any changes in the effort of the force transmitting structure of the bridge. These changes may prove to be disadvantageous to the whole structure because of torsional moments that additionally load the treadways. Giving careful consideration to such operational instances has been highly appreciated because of the possibility of using this kind of bridges while organizing the crossing for vehicles featured with various wheel/track spaces (different from those used previously). The BLG bridge was numerically analysed to assess displacements and distributions of stresses throughout the bridge structure in different loading modes. Because of the complexity of the structure in question and simplifications assumed at the stage of constructing geometric and discrete models, the deformable 3D model of the scissors-type bridge needs verification. Verification of the reliability of models was performed by comparing deflections obtained in the different load modes that corresponded with tests performed on the test stand. It has been shown that the examined changes in conditions of loading the treadways of the bridge are of the greatest effect to the effort of the area of the joint which is attached to the girder bottom. Stress concentrations determined in the analysis are not hazardous to safe operation of the structure.

Key words: scissor-AVLB type bridge, experimental test, numerical FE analysis.

1. Introduction

The paper has been intended to present a numerical analysis of the strength of a scissors – AVLB type bridge (Armoured Vehicle-Launched Bridge). A single-span scissors-type BLG (a manufacturer's designation) bridge manufactured under license in Poland was subject to analysis. A single-span module of such a bridge consists of two structural members (i.e. a ready-made roadway/two treadways and a supporting structure) joined with a coupling pin [1]. The bridge span is extended automatically by means of a mechanical bridge-laying gear carried together with bridge sections on a self-propelled chassis (Fig. 1). The bridgelaying vehicle has been designed to provide immediate deployable bridge capability. The bridge length available is up to 20 m and the load bearing capacity is of 500 kN. The bridges offer obstacle/gap-crossing capability to tracked and wheeled vehicles.

In connection with the BLG-60 bridge modernization (bridge deck widening), there arose the need to conduct basic engineering analyses in order to verify the structure's correctness. Considering the fact that the structure of a BLG bridge is a typical thin-walled one of a complex internal structure [2], innovative engineering systems (CAD/CAE) were implemented in analyses.

Fig. 1. A view of the tested BLG bridge during the deployment process, the stand intended for tests and examinations of BLG bridge that is deployed to a crossing position

*e-mail: malachowskij@wat.edu.pl

On the basis of an electronically reproduced structural documentation of a BLG bridge and a geometric model that was worked out afterwards, a rigid numerical model was created. The model was used to assess the reliability of the structure's operation during the bridge deployment process as well as in determining forces and reactions in the structure's bearings and joints [3].

A deformable numerical model, which is used for assessing displacements and the distribution of stresses in the structure [4] was created in the next phases of the works. In order for the numerical model to be a credible source of information, it is necessary to test its correctness by comparing the results obtained by means of numerical analyses with the results obtained by conducting experiments on an actual object. Field tests on an actual object were carried out and the reliability of the numerical model was verified by means of comparing deflections for the operating load.

2. Experimental load test of BLG bridge

Field tests on an actual structure of a BLG scissors-type bridge were performed in Military Engineering Works. A fully efficient BLG bridge that underwent a general overhaul in Military Engineering Works was used for that purpose (see Fig. 1). The bridge was deployed to a crossing position on a test stand intended for tests and examinations of bridge structures that are repaired, modernized and produced in Military Engineering Works. The test stand in the form of a dry pool with concrete abutments located on the premises of Military Engineering Works is illustrated in Fig. 1.

Prior to beginning actual load tests on a span of the BLG bridge, a test drive of a BLG tracked carrying chassis onto the bridge span laid on concrete pool abutments was realized (see Fig. 2). The purpose of the operation was to initially locate metal anchorages built at the bottom of the abutments of the bridge girders on pool edges under the influence of an external load. Once the chassis/carrier had left the bridge span, it was performed a calibration of the measuring apparatus that corresponded with the state of being loaded only by the deadweight of the span structure. Subsequently, load tests on the BLG span were performed. A BLG tracked carrying chassis without the transported span constituted load in this test. A vehicle in such a configuration, which is presented in Fig. 2, has a mass of 33.3 tons.

After the vehicle had driven onto the bridge, it moved to the mid-length of the bridge. The traces of the contact between caterpillar tracks and the bridge span at the point where the vehicle had stopped are marked in Fig. 2. Measurements that describe the locations of the edges of caterpillar tracks in relation to the edges of the tested bridge treadway are also provided in Fig. 2.

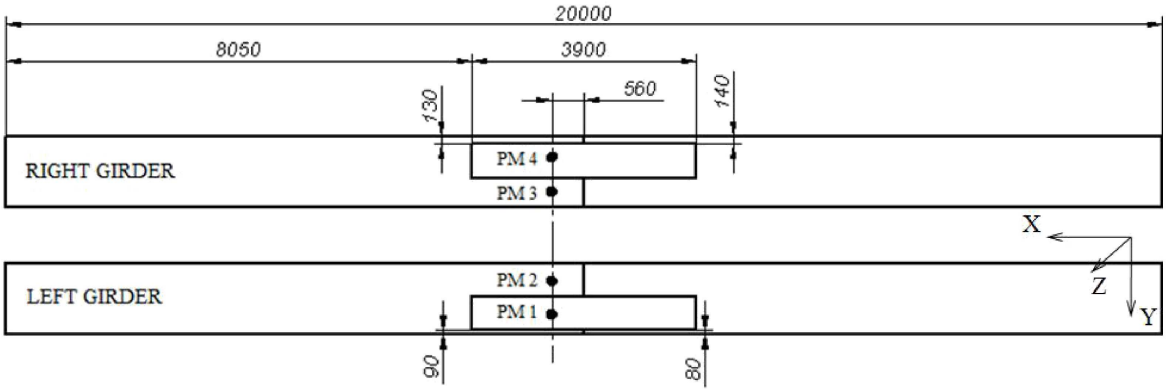

Fig. 2. A BLG tracked carrying chassis without the transported span during the load test and a schematic of the location of the contact between caterpillar tracks and the bridge span at the point where the vehicle had stopped; PM 1-4 – points of measure

For measuring the bridge deflections, two mechanical indicators were used. The indicators were placed at the bridge span's mid-length under the lug of the main joint. A view of such an indicator prepared for measuring dislocation in the axis of the main joint as well as its location can be observed in Fig. 3. The indicator has a slip-ring which, once the structure has been unloaded, is blocked in the final position that has been reached and indicates the value of deflection directly on a scaled sleeve.

In addition to span bending, there simultaneously occurred girders' torsion during both a normal operation of the scissors-type bridge and a load test conducted on the test stand. The presence of an additional load in the transverse plane of the tested structure is the consequence of the eccentricity of the external load which occurs as a result of the displacement of the center of gravity of the vehicle that crosses the bridge relative to the longitudinal axis of the bridge. The above-described measurement of the deflection alone by means of mechanical indicators makes it possible to assess the operation of the bridge in the plane of longitudinal bending but is insufficient to estimate the torsion of the structure's members which results from imprecise driving of the vehicle across the bridge and the occurrence of the eccentricity of the external load. In order to gather sufficient data and prepare a more complete description of the deformations, four potentiometric indicators (two indicators per each girder/deck of the tested bridge) were additionally used. A schematic of the location of the potentiometric indicators on the right girder as well as the view of them on an actual object is presented in the schematic and the photograph shown in Fig. 3 and schematic that interprets the location of indicators on the left and right girders of the bridge in Fig. 10.

Fig. 3. A view of the location of potentiometric indicators used for displacements measuring

Since indicators were placed on both sides of the girder, the difference between vertical displacements recorded with the use of them will make it possible to assess the torsional deformation of the girder in the analyzed section accurately. It will allow a more precise interpretation and assessment of the correctness of the results of simulations obtained with the use of the numerical model and the actual BLG bridge structure.

Displacement values measured by means of particular potentiometric indicators (Fig. 10) were recorded while the tracked chassis was driving across the bridge. Displacements history in the function of the duration of load action on the bridge is shown in diagram presented in Fig. 4.

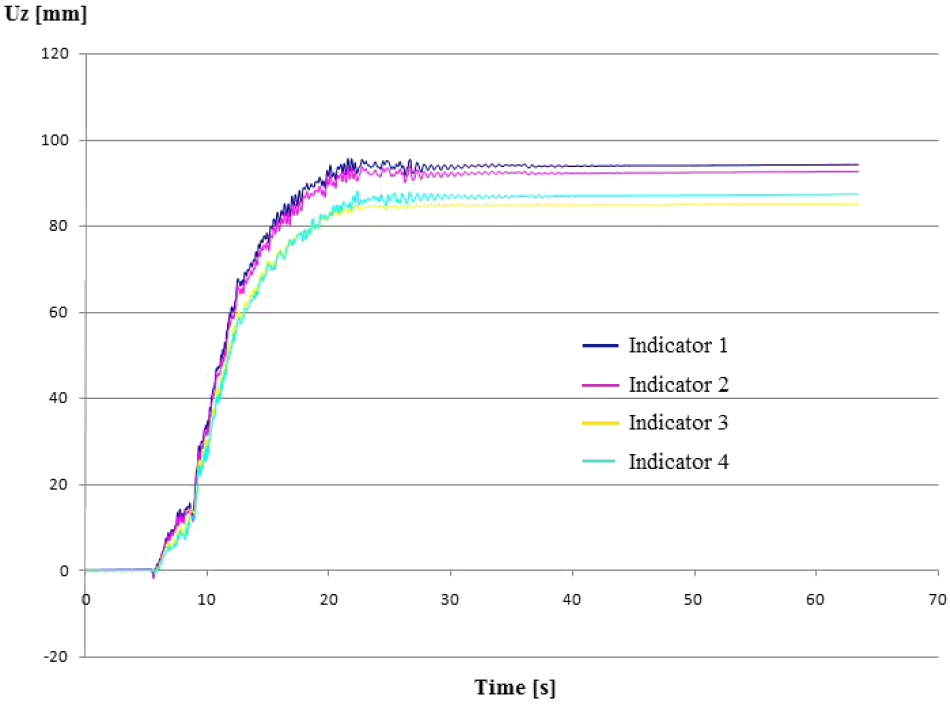

Fig. 4. Vertical displacements vs. time recorded during load test

The maximum deflection value was recorded for the left span and was equal to 94 mm in the analyzed section. The value which was taken from the scale of the mechanical indicator for the left girder was 95 mm. For the right girder, the maximum deflection value measured by means of the mechanical indicator was 87 mm and was equal to the value recorded with the use of potentiometric indicators.

3. Numerical simulation with FE 3D model of the scissors-AVLB type bridge

3.1. Methodology of numerical analysis. A very popular as well as effective and also accurate method of studies on compound constructions is the method consisted in combining experimental and numerical studies. Design offices develop numerical models of new constructions as well as conduct strength analyses. Additionally, strength experimental studies of such a construction or its subsystems are carried out. On the basis of the results of experimental studies, it is possible to verify both a numerical model of the developed construction and the applied calculation method. In case of convergence of the results of both tests, the correctness of the numerical model and the calculation method is verified. The properly developed discrete model can be used for more complicated and complex strength calculations or for modification of the already developed and verified construction. Having the consistent results of numerical and experimental tests obtained for the determined model and determined boundary conditions, it is assumed that while changing boundary conditions or modifying the construction elements, the results of the subsequent numerical analyses will be also correct and reliable. Owing to such an approach, the results of numerical calculations can successfully replace the results of the expensive experimental tests. It is related to the designing process as well as to determination of the reasons of occurrence of the emergency conditions leading even to failure of the important elements of the construction.

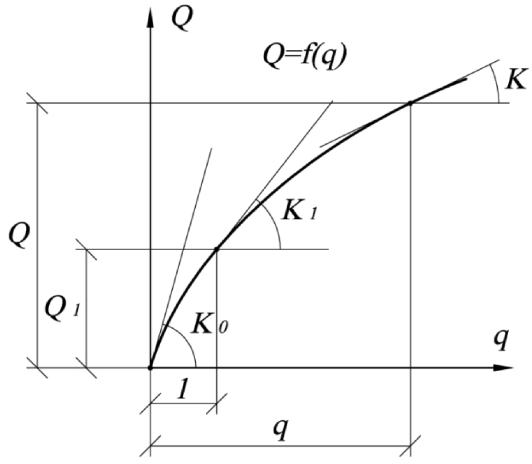

Fig. 5. Nonlinear relation $Q = f(q)$

In the tests on the developed numerical model with nonlinearities resulted from the clearances, the analyses were conducted with the use of an iterative calculation algorithm. The algorithm in question is based on the Newton-Raphson scheme [5, 6] and allows the analysis of the systems with a variable stiffness matrix resulting from the equilibrium state determined by equation $Q = f(q)$, where Q represents the vector of external forces and q is a value of displacement corresponding to it. The scheme in Fig. 5 presents this nonlinearity graphically.

3.2. Numerical model. A discrete model of a single bridge girder was developed with the use of a computer-generated surface model [3] of the BLG structure (Fig. 1). The 3D discrete FE model (see Fig. 6) of a single treadway of a BLG bridge composed of two segments of a girder with a hook-type eye was constructed of surface, solid, and beam elements with the use of a MSC Patran graphic preprocessor [7]. Approximately 75000 shell elements of the QUAD 4 type (4-node element with 24 degrees of freedom) were used in order to represent the structure of internal stiffening members and the skin together with the treadway. Elastic properties of particular elements were described by means of the Young's modulus (a longitudinal modulus of elasticity), E, and the Poisson's ratio, v. Four sets of material parameters were used, assuming that the values of two parameters remained constant in all four sets. The parameters were the Young's modulus, $E = 210000$ MPa, and the Poisson's ratio, $v = 0.25$. Different values of the skin thickness, h, were defined in the FE model as well. The thickness of shell elements depended on which part of the structure was described by the abovementioned elements. Thickness values were in the range: since 4 mm to 11 mm. Members that were precisely represented in the model were as follows: side and bottom skins of the girder segments, structural load-carrying members that make up 34 bulkheads in both segments of the girder including lateral stiffening members (frames and ribs) and longitudinal frame-stiffening members (see Fig. 6).

Movable pin joints between two segments of the girder were defined. The walls of the pin joint were represented in the model in question by means of the elements of the QUAD 4 type, whereas the pin itself was modelled with beam elements of equivalent stiffness determined with the geometric characteristics of the real pin taken from the BLG bridge. Elements that modelled the pin were connected with the central nodes of the mesh of MPC-type (multipoint constraint) elements spread over the edges of the joint's holes. Kinematic relationships between respective nodes of elements, which were intended to represent individual members of the joint, were defined in a way to facilitate rotation of both segments of the girder against each other within the treadway of the bridge. This rotation was limited by the contact joint. The contact area was defined in the roadway area between the girder's segments using GAP-type elements. Another layer of QUAD-type elements was used for modelling the stiffening members used in the actual structure at the bottom of the girder. They were joined with a layer of MPC elements which were used for representing the actual external skin of the girder (see Fig. 6). BEAM (2-node element with 12 degrees of freedom) elements of a properly selected stiffness

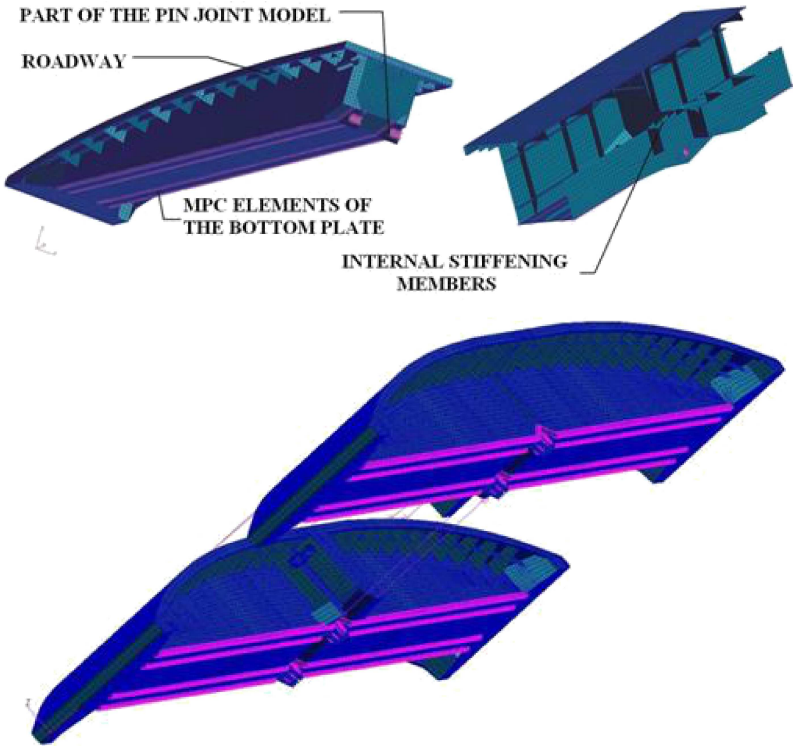

Fig. 6. A 3D numerical model of a single treadway of a BLG bridge, longitudinal section of the girder segment and a complete FE model of a one span BLG bridge

were used as a model of additional stiffening members of the skin of the treadway's limiting edge. The external skin of the roadway made up of plates of the roadway pavement was represented approximately. While modelling that part of the treadway, stiffening mouldings of the treadway reinforcement were ignored. A complete FE model of the one span BLG bridge is shown in Fig. 6. The discrete model of the BLG bridge constructed that way is comprised of 142712 nodes, 143000 QUAD4-type elements, 1312 BEAM-type elements, MPC-type elements and 70 contact GAP-type elements.

3.3. Boundary conditions. On the basis of the analysis of the conditions of deflection measurements, it was found that the bridge span that is laid on concrete abutments on the test stand rests directly on special anchor mandrels that are presented in Fig. 7. The role of the mandrels is to anchor the span in the ground so that the structure is more stable while a tank is driving across the bridge. During conducting the measurement of deflection on the test stand, the mandrels are driven into wooden elements that are laid on a concrete foundation. A necessary simplification was made in analyses, namely, it was assumed that the sections of the fixings of mandrels were the last points of support of the structure at its both ends respectively. In order to represent the above-described situation in a numerical model, constraints were introduced in the rows of nodes that were at a distance of 450 mm from the bridge span. The nodes corresponded with the locations of the fixings of anchor mandrels.

Replacement load was defined in the model by means of distributed load on surfaces on which the caterpillar tracks of the tank adhered to bridge treadways.

A static schematic used in numerical analyses for evaluating deflection of the bridge span is shown in Fig. 7 as well.

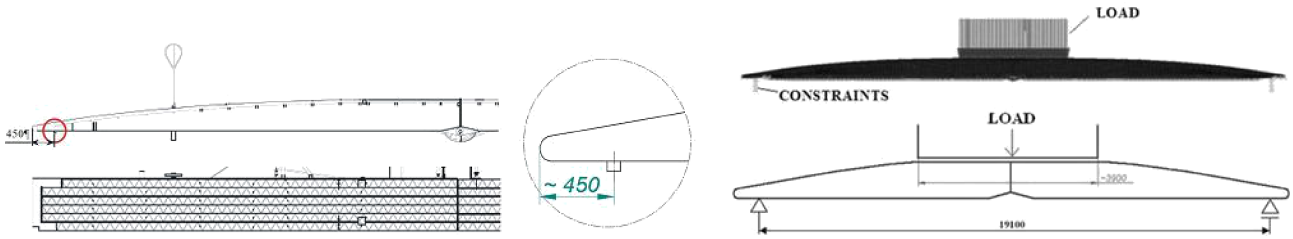

Fig. 7. A schematic of a BLG span treadway with an anchor mandrel and a static schematic for evaluating comparative deflection of the bridge span

4. Results of experimental and numerical studies

A numerical analysis of a single bridge span was conducted with the use of the MSC.Nastran program. The conditions that corresponded with the variant of stand tests described above (Fig. 7) were reproduced. Calculations were performed within the scope of nonlinear statics with accounting for contact phenomena in the mating zone of particular segments of both bridge girders. In the presented variant of the analysis, load that corresponded with the weight of a chassis driving across the bridge was represented in the model. The weight was 33.3 tons. The load was applied in the form of pressure to the surface of the adherence of the caterpillar track to the bridge treadway. Once the vehicle had stopped at the mid-length of the span, it was found that caterpillar tracks were not evenly laid in relation to the bridge axis. Therefore, in the numerical model, it was accounted for the asymmetry of the position of caterpillar tracks in relation to the bridge treadways, which is illustrated in Fig. 2, by distributed load applied to particular elements that modelled the bridge deck.

On the basis of numerical analysis results, deflections for the left and the right bridge treadways were determined. The maximum deflection for the left girder was 87 mm, whereas for the right girder, it was equal to 80 mm. Differences between the maximum displacements of both girders resulted directly from the actual load distribution on the bridge treadways. There occurred a stronger deflection and torsion of the girder in the left treadway, since load was not distributed symmetrically on both bridge decks. Fringe of displacements in both girders is illustrated in Fig. 8.

A correlation of results concerning maximum displacements recorded during experimental tests by means of mechanical indicators as well as results obtained by means of numerical analyses are presented in Table 1.

Maximum displacement values obtained by means of numerical analyses were lower that the values of maximum displacements measured with the use of mechanical indicators. The maximum difference between dislocations was 8.4%. For the right girder, the difference was 8% (Table 1). Deformations of the right girder resulted from simultaneous deflection and torsion and were smaller.

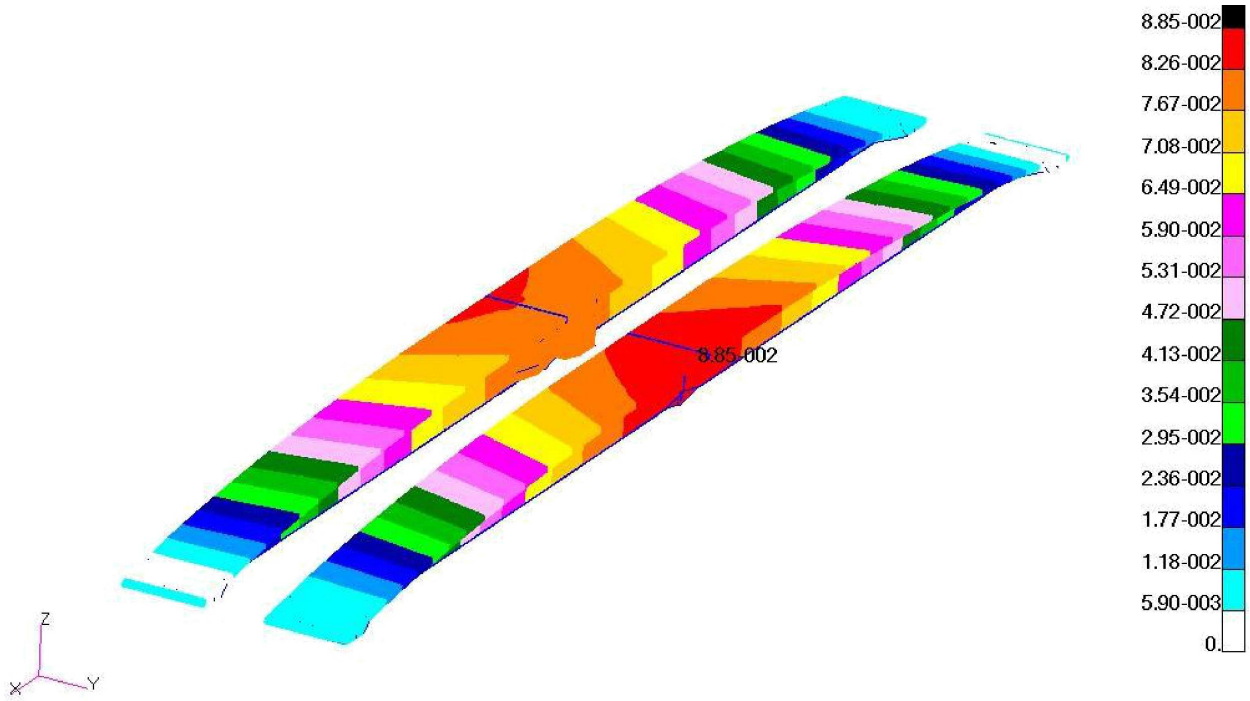

Fig. 8. Fringe of resultant displacements of the bridge span obtained numerically

Table 1
Comparison of the maximum displacements recorded during experimental and numerical tests

	Maximum deflections [mm]		Difference [%]
	Mechanical indicator	FE analysis	
Left girder	95	87	8.4
Right girder	87	80	8.0

Apart from comparing maximum deflections of girders, a comparison of displacement values in the section located at the distance of 560 mm from the main joint axis (Fig. 3) was performed. A correlation of results recorded by means of potentiometric indicators located in measurement sections as well as displacements determined numerically in particular span model sections are presented in Table 2.

Displacement values in tested sections obtained numerically were smaller by approximately 8% than the values of displacements recorded during stand tests. On the basis of the comparison of displacement measurements in the sections of particular girders, it is possible to assess their torsion. After deformation maps obtained by numerical analyses had been compared, it was found that torsion was stronger in the case of the left girder (Fig. 9 and Table 4).

Results obtained by means of potentiometric indicators suggest that the value of torsion was higher for the left girder. However, the discrepancy was insignificant and did not exceed the value of 1 mm. Figure 9 illustrates deformations in the analyzed section for the left girder. Location of measurement indicators as well as maximum values of displacements in the analyzed section are marked in Fig. 9 and Table 4. Numerical studies presented in this part of the work are related to a modernised BLG scissor bridge in which roadways were extended in respect to traditional version of the bridges hitherto exploited in Polish Armed Forces. Such a constructional change significantly affects the effort changes of the bridge components and the forms of deformations of girders.

During the regular exploitation of a scissor bridge as well as during the loading test performed on a testing stand, apart from span bending there also occurs simultaneous girders torsion. Loading with a torsion moment in the transverse plane of the bridge girders largely results from the applied constructional solutions including extended, as a result of modernization, roadways which are significantly extended beyond the girder contour (Fig. 1, 2). It is also caused by the eccentricity of the external load of the bridge span. It occurs as a result of asymmetric position of caterpillars on the bridge roadway and, as an effect, displacement of the centre of gravity of the crossing vehicle in respect to the bridge longitudinal axis. Taking into consideration the strength of construction, applying the loads shifted in respect to the bridge longitudinal axis (outside the contour of the girders-treadways) generates the change of both strain and deformation of the girders of such a construction [8].

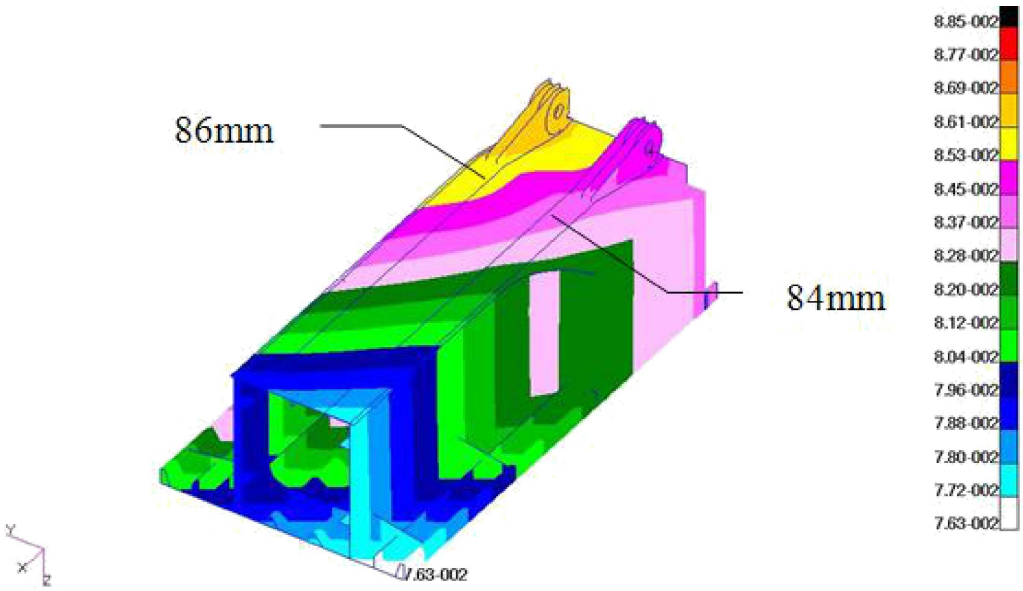

Fig. 9. Deformations in the analyzed section for the left bridge girder

Table 2
Comparison of the displacements recorded in the one section of girder during field and numerical tests

	Vertical displacements [mm]			Difference [%]
	Id of PM	Potentiometric indicator	FE analysis	
Left girder	1	94	86	8.5
	2	92	84	8.7
Right girder	3	84	80	4.8
	4	87	80	8.0

To evaluate the torsion value of the elements of the construction resulted from inaccuracy of placing of the crossing vehicle on the bridge and appearance of the eccentricity of the external load, the measurements of vertical displacement of bottom plate of the girders by means of potentiometric indicators were applied. To gather the essential data and more precise description of deformation including torsion of treadways, four potentiometric indicators, two on each girder of the tested bridge, were applied. The scheme of the potentiometric indicators location under the bottom plates of the right and left girders and their view on the real object are presented in the photo in Fig. 3 and in the scheme (Fig. 10).

Figure 11 presents an isometric view of deformation of cross-sections in the measurement plane and the fragments of girders with maps of magnitude displacements after tenfold calibration of the results obtained in the numerical simulation of the loading test of the span.

Figure 12 presents deformation of both the girders in the plane of cross-sections of the bridge girders in the measurement plane along with the maps of vertical displacements after tenfold calibration. The undeformed cross-sections with colourful maps of vertical displacements were used to present the deformed cross-sections of the left (marked L in Figs. 11 and 12) and the right – R girder of the span loaded in FE model. In this figure, there are clearly visible not only vertical displacements related to bending in the longitudinal plane but also rotations related to torsion of the construction.

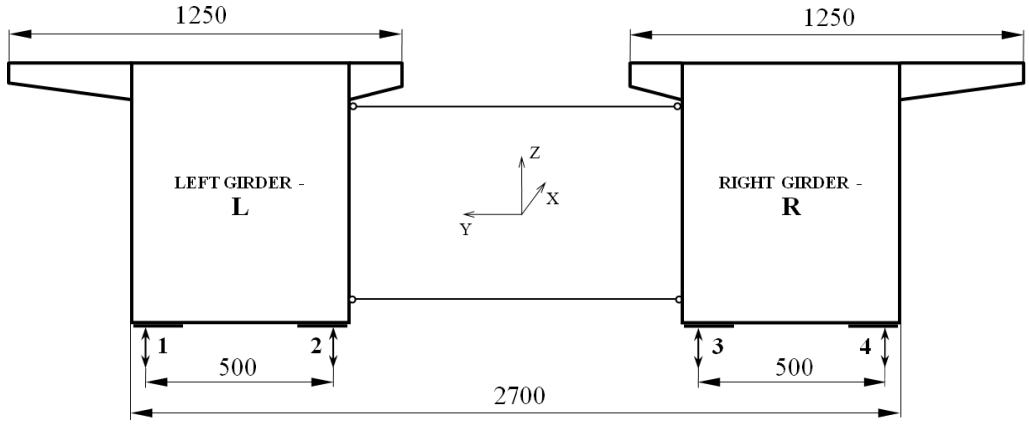

Fig. 10. Scheme of distribution of potentiometric indicators -1, 2, 3, 4 (displacements measurement points) on the reinforcements in the planes of lower girders

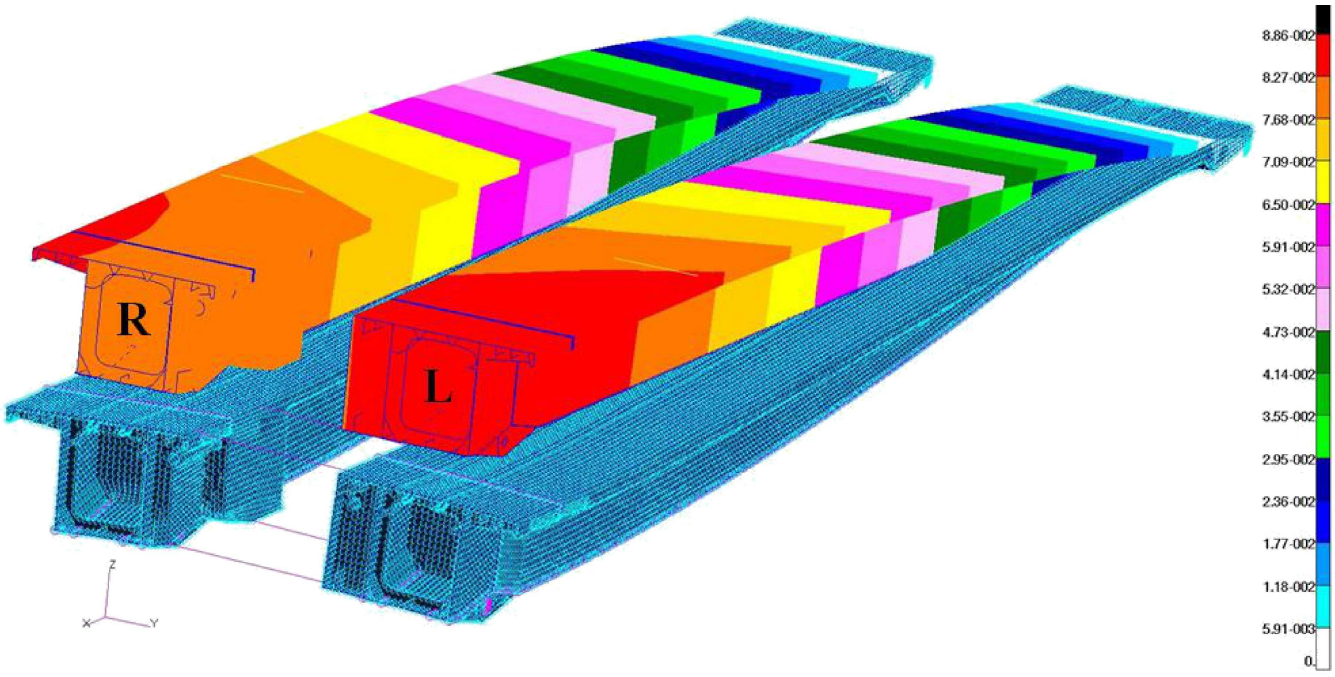

Fig. 11. Isometric view of deformation of cross-sections in the measurement plane and the fragments of girders with maps of magnitude displacements (tenfold calibration) $-U_{\max} = 88.6$ mm

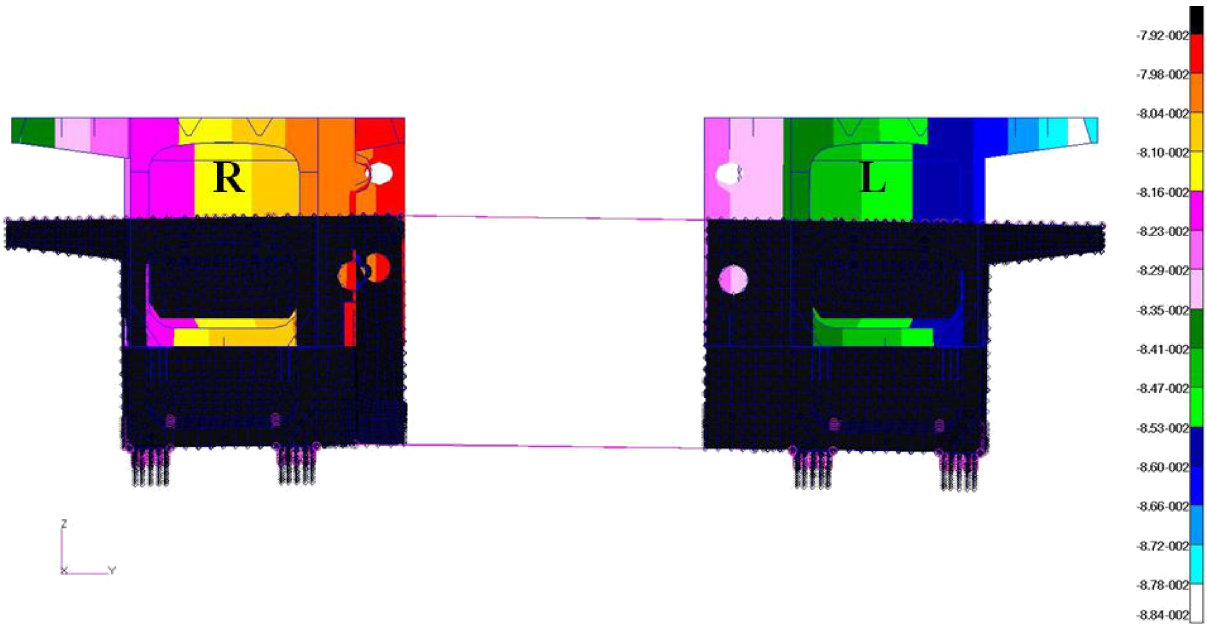

Fig. 12. View of deformation of cross-sections of girders in the measurement plane with maps of vertical displacements (tenfold calibration) $-U_{Z\,\max} = -88.4$ mm

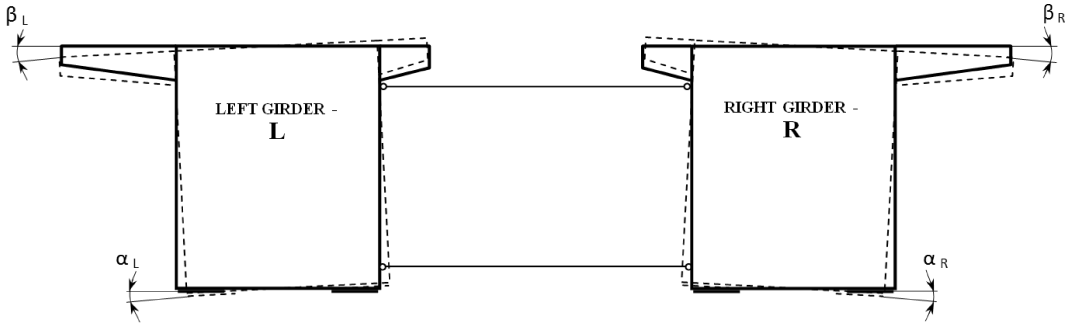

Fig. 13. Scheme of deformation of cross-sections of the bridge girders in the measurement plane

The girders torsion angles of the real construction during loading test were determined analytically based on the difference of vertical displacements of the bottom plates recorded by means of potentiometric indicators: 1–2 for the left girder and 3–4 for the right girder, as shown in Fig. 10. The same methodology of determining the torsion angles α_L and α_R of the girders bottom (Fig. 3 and Fig. 13) was applied to numerical tests. In this case, there were used vertical displacements determined in the numerical model of the span in appropriate cross-sections corresponding to the points of experimental measurements on the bottom plates. Torsion angles β_L and β_R in the plane of roadways of both the girders (Fig. 13) were determined based on the differences of vertical displacements of the outer edges of roadways determined numerically. The tests assumed that the influence of torsion of cross-sections of ending supporting elements on deformation of the span is insignificant due to the manner of supporting the real span on the concrete bridgeheads during the loading test.

The values of torsion angles of girders bottom plates determined based on the results of experimental measurements and numerical tests are compared in Table 3 (values of angle defined in minutes [']). The maximum values of torsion angles of the girder bottom are less than 1°. The maximum relative differences of torsion angles determined based on the numerical results and experimental tests are approximately 12% in the right girder and 40% in the left girder.

Table 4 compares the values of torsion angles of the girders walls determined based on the numerical results in the plane of roadways of both the girders. A larger angle was obtained in the plane of the left girder. The maximum relative difference of torsion angles of treadways determined numerically in the plane of roadways of both the girders is approximately 12%. The absolute values of torsion angles of treadways determined numerically in the plane of the roadway are slightly smaller than the values of torsional angles determined in the girders bottom walls and are respectively: 0.9' in the left girder and 2.5' in the right girder.

Table 3
Comparison of values of torsion angles of girders in the plane of bottom plates

	Torsion angle left girder α_L [']	Torsion angle right girder α_R [']	Absolute difference of torsion angles $\lvert\alpha_L - \alpha_R\rvert$[']
Field tests	11.2	14.0	2.8

Table 4
Comparison of values of torsion angles of the girders determined numerically in the plane of the roadway

	Torsion angle left girder β_L [']	Torsion angle right girder β_R [']	Absolute difference of torsion angles $\lvert\beta_L - \beta_R\rvert$ [']	Maximum relative difference of torsion angles $\Delta\beta_{\max} = \lvert(\beta_{\max} - \beta_{\min})/\beta_{\min}\rvert$ [%]
Numerical analysis	14,8	13.2	1.6	12.3

The decks of bridge roadways were widened in connection to the modernization process. The free parts, particularly the outer edges of roadways, are deformed stronger than the rest of the girders cross sections. Vertical displacements of the outer edges of roadways were determined numerically to assign torsion angles β_L and β_R in the plane of roadways of both the girders (Fig. 13). It may be a reason that the maximum relative difference of torsion angles, determined numerically in the plane of the roadway, is approximately 12%.

5. Conclusions

Load tests performed on a modernized BLG bridge structure made it possible to verify the reliability of numerical models, which are used for assessing the stress distribution in the analyzed structure as well as analyzing the bridge in different configurations in special uses, taking crisis situations into particular consideration. Verification of the reliability of models was performed by comparing deflections obtained in a load mode that corresponded with the test performed on the test stand. Displacements were measured by means of mechanical indicators located in the section that corresponded to the half-length of the bridge, and by means of potentiometric indicators located in the selected section of a girder. In the considered load case, the maximum difference between experimental results and the results obtained numerically was approximately 9%.

An application of the results of measurements of vertical displacements of girders bottom plates by means of potentiometric indicators enabled determination of the base value of the girder torsion deformation in the span measurement cross-section. The comparative tests of torsion deformation defined during the load test and determined numerically enable more precise interpretation of the response of the span subject to test load and estimation of the accuracy of both the numerical model mapping the BLG bridge construction and FEM simulation results.

The numerical analysis and tests presented in the paper do not take into consideration the clearances in pivot joints of the real construction. The clearances may vary in both of the girders joints. They influence on bending inequality and on torsion bridge girders as well. The elimination of the clearances in the pivot joints under the influence of external loads causes additional inelastic bending and span girders torsion. They may influence on the differences in the results determined in numerical analyses and recorded during field tests.

It was verified that the manner of mapping the real boundary conditions and internal constraints in numerical models significantly influences the correctness of the calculation results. In the subsequent stages of works, it is planned to carry out the comparative analysis in the particular cross-sections of the construction and selection of an optimal manner of mapping the supporters including the ground susceptibility and loads in numerical models for numerical analyses of BLG bridge in different constructional configurations.

On the basis of the conducted tests, it was found that the way of reproducing actual boundary conditions in numerical models has a great effect on the reliability of computations. In next stages of the work, it is planned to conduct a comparative analysis of stresses in particular sections of the structure as well as to select an optimal way of reproducing bearings and loads in models used for numerical analyses of the BLG bridge in different structural configurations.

REFERENCES

[1] Ministry of National Defence in Poland, "Military bridges", *MND Manual*, MND, Warsaw, 1994, (in Polish).

[2] Ministry of National Defence in United Statets, "Trilateral designe and test code for military bridging and gap-crossing equipment", *Operational Manual*, MND, New York, 1996.

[3] W. Krason and L. Filiks, "Rigid and deformable models in the numeriacal strength tests of scissor bridge", *WAT Bulletin* LVII 2 (650), 103–116, (2008), (in Polish).

[4] W. Krason and M. Wieczorek, *Strength of the Floating Bridges – Computer Aspect*, p. 269, Military University of Technology, Warsaw, 2004, (in Polish).

[5] G. Rakowski and Z. Kacprzyk, *Finite Element Method in Mechanics of Structures*, Warsaw University of Technology Publishing House, Warsaw, 1993, (in Polish).

[6] E. Rusinski, J. Czmochowski, and T. Smolnicki, *Advanced Finite Element Method for Load-carrying Structures of Machines*, Wroclaw University Press, Wroclaw, 2000, (in Polish).

[7] MSC Sottware, *MSC Reference Manual*, "MSC Patran/Nastran, Version r2", MSC. Software, New York, 2005.

[8] L. Czechowski and T. Kubiak, "Analysis of thin-walled girders subjected to a pulse torsional torque", *J KONES Powertrain and Transport* 19 (1), 51–62 (2012).